UDK/*UDC*: 622.515:624.13
Izvirni znanstveni članek – *Original scientific paper*
DOI: 10.15292/acta.hydro.2026.06

Prejeto/*Received:* 28.04.2026
Sprejeto/*Accepted:* 07.09.2026
Objavljeno na spletu/*Published online:* 20.11.2026

EFFECT OF A SOIL CAVITY ON THE HYDRAULIC CHARACTERISTICS OF A SATURATED FLOW UNDER A HYDRAULIC STRUCTURE

VPLIV VOTLINE V ZEMLJINI NA HIDRAVLIČNE ZNAČILNOSTI NASIČENEGA TOKA POD HIDROTEHNIČNIM OBJEKTOM

Ihsan A. Abdulhussein[1,*], Rafi M. Qasim[1], Saja M. Naeem[1], K.S. Hari Prasad[2]

[1]Basrah Engineering Technical College, Southern Technical University, Basrah, Iraq

[2]Department of Civil Engineering, Indian Institute of Technology, Roorkee, India

Abstract

This study involved developing a mathematical model to simulate saturated flow beneath hydraulic structures, including dams, barrages, and canal regulators, utilizing the finite difference method. This model is used to calculate the critical hydraulic properties under hydraulic structures, such as the uplift pressure head exerted on the hydraulic structure, the amount of discharge downstream, under-seepage, and the exit gradient. The hydraulic properties under the hydraulic structure were analyzed for the presence and absence of a single cavity. The effect of cavity size and location on the hydraulic properties of seepage under the hydraulic structure was investigated. The difference value for each of the hydraulic properties between the presence and absence of a single cavity was calculated. The results indicate that the presence of a single cavity in the problem domain leads to a reduction in the exit gradient, downstream discharge, and uplift pressure head. Meanwhile, the bottom leakage exhibited a non-linear response (a decrease or increase) depending on the spatial coordinates of the cavity. The study further analyzed the effect of a borehole downstream of the hydraulic structure apron on relieving the influence of the cavity on the under-seepage discharge. The study of a single cavity helps guide maintenance operations by accurately determining the coordinates of grouting operations and classifying the risk of leakage in existing structures based on the extent of soil erosion. In doing so, it provides engineers with criteria for the early detection of infrastructure defects, thereby contributing to the updating of international standards and ensuring the sustainability of dams in geotechnically complex locations.

Keywords: seepage, hydraulic structure, uplift pressure head, cavity, boreholes, numerical modeling.

---

[*] Stik / *Correspondence*: drengihssan@stu.edu.iq

© Abdulhussein I. A. et al.; This is an open-access article distributed under the terms of the Attribution-ShareAlike 4.0 International (CC BY-SA 4.0) licence.

© Abdulhussein I. A. et al.; Vsebina tega članka se sme uporabljati v skladu s pogoji licence Priznanje avtorstva-Deljenje pod enakimi pogoji 4.0 Mednarodna (CC BY-SA 4.0).

Izvleček

Raziskava preučuje razvoj matematičnega modela za simulacijo nasičenega toka pod hidrotehničnimi objekti, vključno z jezovi, pregradami in zapornicami, z uporabo metode končnih razlik. Model se uporablja za izračun kritičnih hidravličnih lastnosti pod hidrotehničnimi objekti, kot so vzgonski tlak, ki deluje na hidrotehnični objekt, količina dolvodnega pretoka, podtekanje in izstopni gradient. Hidravlične lastnosti pod hidrotehničnim objektom so bile analizirane za primer prisotnosti in odsotnosti ene same votline. Preučevali smo vpliv velikosti in lege votline na hidravlične lastnosti pronicanja pod hidrotehničnim objektom. Izračunali smo razliko v vrednostih posameznih hidravličnih lastnosti pri prisotnosti in odsotnosti ene same votline. Rezultati kažejo, da prisotnost ene same votline v obravnavanem območju vodi do zmanjšanja izstopnega gradienta, dolvodnega pretoka in vzgonskega tlaka. Hkrati je precejanje skozi dno pokazalo nelinearni odziv (zmanjšanje ali povečanje) glede na prostorske koordinate votline. Raziskava je preučila tudi vpliv vrtine dolvodno od podslapja na vpliva votline na pretok podtekanja. Proučevanje posamezne votline pomaga pri usmerjanju vzdrževalnih del, saj omogoča natančno določitev koordinat injektiranja in razvrščanje tveganja za precejanje v obstoječih objektih glede na obseg erozije tal. S tem inženirjem zagotavlja merila za zgodnje odkrivanje poškodb infrastrukture, s čimer prispeva k posodobitvi mednarodnih standardov in zagotavljanju trajnosti jezov na geotehnično zahtevnih lokacijah.

Ključne besede: precejanje, hidrotehnični objekt, višina vzgonskega tlaka, votlina, vrtine, numerično modeliranje.

1. Introduction

One significant challenge in hydraulic structures is the issue of seepage and uplift pressure, which can lead to problems such as piping, internal erosion, overturning, and sliding beneath these structures. A major challenge encountered on site,which affects the stability of hydraulic structures such as dams, barrages, and regulators, relates to the presence of cavities. These cavities dominate the quantity of seepage, uplift pressure, and exit hydraulic gradient. Also, cavities lead to the collapse of the hydraulic structure in some cases, so their existence in homogeneous and non-homogeneous soil must be considered in design and analysis calculations, and assessed correctly to avoid damage to hydraulic structures. Maatooq et al. (2014) performed an experimental study to derive an empirical equation for determining the extent of seepage under sheet pile walls. The cavity's presence was taken into consideration. Their equation was derived from 33 tests. Baena and Toledo (2014) conducted a study aimed at modeling the seepage progression caused by the dissolution of soluble particles within dam foundations. They utilized a numerically validated experimental model to simulate the dynamics of intergranular flow and dissolution. The findings revealed a significant rise in the permeability of the foundation soil as the subsurface cavity gradually enlarges over time. Experimental research by Abdallah (2017) explored the effect of cavities on the stability of the dam in the presence of water flow. The results determined the best sheet pile location in the presence of cavities at various vertical and horizontal locations. Nadhir et al. (2017) conducted a study that simulated the expansion of cavities within karst formations, with a particular focus on the hazards associated with the Mosul Dam site. That research aimed to assess the risks posed by ongoing void formation in soluble rocks, such as gypsum, to the safety of the dam. Findings from the study underscored that concealed voids significantly increase the risks of internal erosion and the potential for foundation failure. Jamel and Ali (2018) studied a hydraulic structure model with an upstream sheet pile based on *SEEP/W* software. Various results were found for discharge, exit gradient, and uplift pressure. A dimensional analysis was employed to study the impact of these hydraulic variables. Equations for discharge, exit gradient, and uplift pressure were obtained. When a cavity was located before the sheet pile, it had a greater impact on the discharge and uplift pressure, and when the cavity was near the end of the structure, it had a greater impact on

the exit gradient. As well, decreasing the cavity depth from the ground surface increases its effect on the seepage characteristics. The cavitation diameter and a greater coefficient of permeability also increase seepage properties. Aziz and Abdallah (2018) carried out an experimental study to assess the seepage characteristics. Their model was composed of a dam and sheet pile fixed at various locations (at the dam's heel, mid-span, and toe). The model was supported by sandy soil, which included cavities at various positions and directions. By adopting the experimental work, about thirty-three tests were conducted in the laboratory to determine seepage amount and flow line direction. It was found that the suitable location of sheet pile at the toe of dam considering cavity with Xc/B=0 and 0.5 while that the suitable location of sheet pile at the heel of dam considering cavity with $Xc/B \geq 1$, where Xc is the horizontal distance from upstream sheet pile to the cavity and B is the length of the hydraulic structure. Also, when the cavity is located upstream, the optimal position for the sheet pile wall is at the midpoint of the dam floor. Maatooq and Abdulhasan (2019) investigated experimentally the seepage amount and the uplift pressure under a hydraulic structure in homogeneous soil, which contains a single cavity at a certain position. The data were evaluated in order to develop deterministic equations for determining seepage and uplift pressure head. The results indicate that having a cavity on the upstream side positively influences seepage behavior by lowering the maximum uplift pressure and reducing the exit hydraulic gradient. When the cavity was present on the downstream side, the influence became negative, except in a few areas. Ali and Tanaka (2023) investigated the hydraulic effects of varying cavity locations on seepage through dam foundations. Utilizing Finite Element Method (FEM) numerical analysis, they simulated multiple spatial configurations. Their findings reveal that cavities situated on the upstream side significantly increase seepage rates compared to those found downstream. Hameed et al. (2025) conducted a study to assess the performance of zoned earth dams under both static and seismic conditions in the presence of foundation cavities. Their approach integrated a 1:25 scale physical model tested on a shaking table with numerical simulations utilizing SEEP/W and QUAKE/W. The results indicated that configurations with upstream and double cavities resulted in the most severe deformations, characterized by notable crest displacement and subsidence. These configurations also led to elevated pore pressures and a significant increase in seepage rates. In contrast, cavities located downstream had a minimal effect on the dam's structural integrity. The study underscores the importance of cavity geometry and positioning as critical factors influencing dam safety. In the present study, a comparison was performed between the effects of the presence and absence of a single cavity within the soil on the hydraulic properties of seepage below the hydraulic structure. Also under study is the effect of drilling a borehole in the downstream floor of the hydraulic structure on relieving the effect of the cavity on the under-seepage discharge.

2. Numerical model and hydraulic gradient computations

Consider the problem of two-dimensional seepage through homogeneous anisotropic porous media under a hydraulic structure as shown in Figure 1. The soil particles and the fluid in the pores are considered incompressible. The equation (Bear, 1979) that describes the flow through a saturated porous medium is:

$$K_x \frac{\partial^2 H}{\partial X^2} + K_y \frac{\partial^2 H}{\partial Y^2} = S_s \frac{\partial H}{\partial t} \quad (1)$$

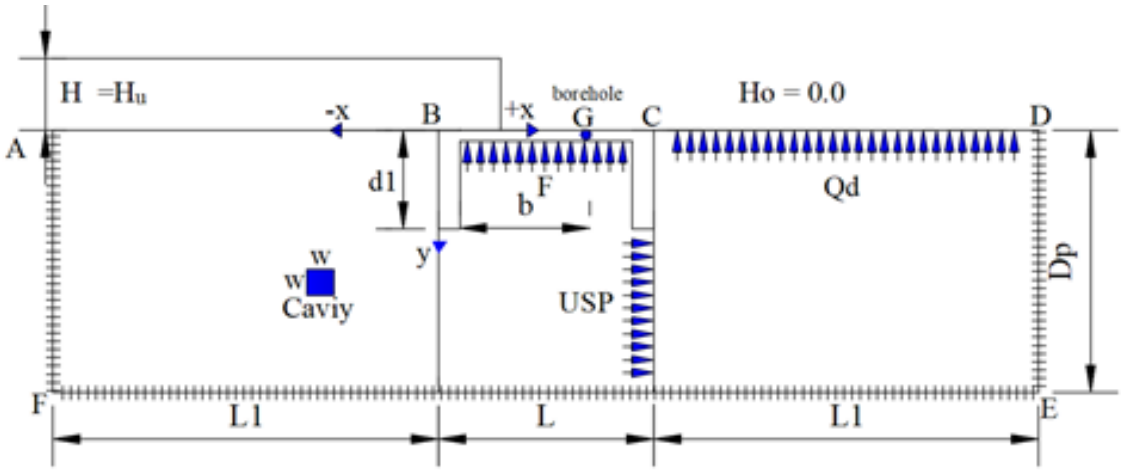


Figure 1: *Problem domain and boundary conditions.*

Slika 1: *Obravnavano območje in robni pogoji.*

where *Kx* and *Ky* are the hydraulic conductivity in the *X* and *Y* directions, respectively. *H* is the piezometric head, *t* is the time, and *Ss* is the specific storage, which is equal to zero for a steady-state condition. Figure 1 illustrates the hydraulic structure floor, characterized by a length *L* and featuring two identical sheet piles, *d1*, positioned upstream and downstream. A borehole may be situated at any point between these sheet piles, specifically at a distance *b* from the upstream sheet piles. The flow domain is constrained by a maximum depth of *Dp* and extends a limited distance from both the upstream and downstream sheet piles, denoted as *L1* and *L2*, respectively. The piezometric heads at the upstream and downstream ends are represented as *Hu* and *Ho*. The boundary conditions for this problem are as follows (Figure 1):

$H = H_u$ on face A-B (2a)

$H = H_o$ on face CD (2b)

$H_b = H_o$ on borehole (2c)

(i.e. the piezometric head is specified)

$K_y * \frac{\partial H}{\partial Y} = 0$ on face E-F, B-C (2d)

(i.e. the velocity component normal to the horizontal boundary is zero)

$K_x * \frac{\partial H}{\partial X} = 0$ on A-F, D-E (2e)

(i.e. the velocity component normal to the vertical boundary is zero).

A numerical model has been developed using the finite difference method by solving equation (1) subjected to the boundary conditions (equation 2a). The resulting system of equations is solved using the Iterative Alternating Direction Implicit Explicit (AIDIE) scheme (Remson et al. 1971). AIDEI is a numerical differential method that solves groundwater flow equations by alternating between implicit and explicit directions, thereby decoupling the problem and transforming large matrices into simple systems that are efficiently solved using the Thomas algorithm. This method is characterized by its unconditional stability and high accuracy, which reduces computational complexity and allows for the modelling of seepage distribution around cavities at low cost. Although it requires a regular grid as an engineering constraint, it remains an effective tool that combines the stability of implicit methods with the simplicity of explicit ones to ensure the accuracy of hydraulic analysis beneath structures. This model calculates the spatial and temporal piezometric heads at each node within the defined domain (Figure 1). The problem domain is discretized to 41 rows and 151 columns, resulting in a total of 6,191 nodes formed at the intersections of these rows and columns. The spacing between both rows and columns is uniform. The solution is

obtained by establishing specific criteria. The variations in the computed piezometric head values between two consecutive iterations for all nodes are aggregated. This total is then evaluated against a predetermined convergence factor, referred to as *E1*. The *ADIE* iterations continue until this sum falls below the value of E1. In this study, *E1* is set at 0.001.

From these piezometric heads, the hydraulic gradient at each node is determined as follows:

$$i = \frac{dH}{dS} \tag{3}$$

where *i* is the hydraulic gradient and *S* is the distance along the flow streamline.

The non-dimensional geometry variables, along with their respective values and ranges, are detailed in Table 1. This set of variables was utilized for conducting all test runs in the study.

Table 1*: Details of the non-dimensional geometry.*

Preglednica 1: *Podrobnosti brezdimenzijske geometrije.*

Variable	Symbol	Values / Range
Upstream water head	H/L	0.12, 0.16, 0.20
Cavity size	W/L	0.02, 0.03, 0.04
Horizontal distance	X/L	−0.74 to 1.86
Vertical distance	Y/L	0.14, 0.34, 0.54
Borehole location	b/L	0.32, 0.52, 0.72

3. Methodology

The solution to equation (1) and the boundary conditions in equations (2-a) to (2-e) for steady-state flow give the value of the piezometric head at all points of the problem domain. The uplift pressure head can be determined by multiplying the computed piezometric head by the unit weight of water. The resultant total uplift pressure head can be calculated by computing the area of the uplift pressure head distribution diagram under the apron of the hydraulic structure. Also, by the derivation of the piezometric head, the hydraulic gradient can be determined, as explained in equation (3), and then the discharge velocity and the flow amount for any section of the domain can be obtained. The amount of discharge for downstream, upstream, cavity, and under-seepage is determined by computing the normal hydraulic gradient along the downstream or upstream bed, and along the cavity boundaries, then employing numerical integration. Thus, the following can be calculated:

- The resultant uplift pressure head acting on the hydraulic structure apron *F*.
- The exit gradient at the end of the downstream apron *EG*.
- Amount of downstream discharge *Qd*.
- Amount of under-seepage discharge *USE*.

The effect of cavity size and location on the aforementioned hydraulic properties is presented. Each of the hydraulic properties was calculated for cases with and without the cavity, and this difference was related to the cavity location. The equations describing the relative change in uplift pressure head, exit gradient, downstream discharge, and under-seepage discharge are as follows:

$$\Delta F = \frac{F_c - F_w}{F_w} \tag{4}$$

$$\Delta EG = \frac{EG_c - EG_w}{EG_w} \tag{5}$$

$$\Delta Qd = \frac{Qd_c - Qd_w}{Qd_w} \tag{6}$$

$$\Delta USE = \frac{USE_c - USE_w}{USE_w} \tag{7}$$

where indices *w* and *c* mean values for cases without and with a cavity, respectively. Thus, a relationship can be drawn for each of the above attributes, from which it is possible to predict the effect of a cavity for various locations under the hydraulic structure. A cavity under a hydraulic structure can be represented numerically using a very high value of hydraulic conductivity. No prior research has definitively established the relationship between the hydraulic conductivity of the cavity *Kc* and that of the underlying subsoil *Ks*. To identify an appropriate ratio for this investigation, one of the mathematical numerical models mentioned in item 2 above was employed with various hypothetical ratios. The findings, detailed in Table 2, highlight the relative change in hydraulic properties such as downstream discharge *ΔQd*, exit gradient *ΔEG*, and resultant uplift head *ΔF*. Notably, cavitation effects are significant at

ratios of 1,000 and higher, while their influence diminishes at ratios exceeding 250,000. Additionally, it was noted that the relative change of all hydraulic property values decreased irrespective of the *Kc/Ks* ratio applied. Consequently, a ratio of 150,000 was chosen for this study, as it serves as a balanced representation between the ratios that affect hydraulic properties.

Table 2: *The relative change in hydraulic properties for different values of Kc/Ks; X/L=0.46, W/L=0.04, Y/L=0.54, and H/L=0.16.*
Preglednica 2: *Relativna sprememba hidravličnih lastnosti za različne vrednosti Kc/Ks; X/L=0,46, W/L=0,04, Y/L=0,54 in H/L=0,16.*

Kc/Ks	ΔQD	ΔEG	ΔF
1	0.000	0.000	0.000
10	-0.003	-0.004	0.000
100	-0.003	-0.005	0.000
1000	-0.001	-0.002	-0.002
10000	-0.030	-0.032	-0.029
50000	-0.239	-0.191	-0.184
100000	-0.333	-0.368	-0.290
150000	-0.620	-0.538	-0.554
250000	-0.613	-0.678	-0.530
500000	-0.614	-0.680	-0.532
1000000	-0.615	-0.680	-0.532

4. Solution in Terms of Stream Function

For steady-state conditions, the governing equation in terms of stream function Ψ is as follows:

$$\frac{\partial^2 \Psi}{\partial X^2} + \frac{\partial^2 \Psi}{\partial Y^2} = 0 \qquad (8)$$

The same finite difference technique with appropriate boundary conditions was used to obtain the stream function distribution of the problem domain. The floor profile BC, as shown in Figure 1, forms the inner boundary of the upstream flow and can thus be taken as the streamline, $\Psi=0$. The outer impervious boundary forms another streamline, $\Psi=Q_T$, in which Q_T = total discharge seeping from the upstream side. The value of Q_T is determined by computing the normal hydraulic gradient along the upstream bed and then employing numerical integration. For boreholes, the foundation profile GC forms the inner boundary of downstream flow and may be taken as a streamline $\Psi=Q_B$, in which Q_B is the total discharge per unit width drained through the boreholes. The value of Q_B is determined by computing the normal hydraulic gradient at the boreholes (Cedergreen, 1989).

5. Results and Discussion

The finite difference solution is used to determine the pressure heads and hydraulic gradients. The findings from the finite difference model have been corroborated with experimental data provided by Chawla (1976). A comparison is presented in Table 3, which contrasts the solutions from the finite difference model with the experimental results for simplified scenarios. This table highlights the pressure head ratio (H/Hu) for cases involving both the presence and absence of a borehole. The results indicate a strong alignment between the two sets of solutions. The pressure heads are used to plot the equipotential lines, whereas the discharge that is obtained from numerical integration of the hydraulic gradient is used to plot the streamlines. Figure 2 shows the equipotential lines for the case of flow without cavity and boreholes, with cavity, and with cavity and boreholes. This figure is plotted using constant values for the upstream head ratio *H/L*, cavity size *W/L*, cavity location *Y/L*, and borehole location *b/L* for comparison purposes. It is clear from this figure that the presence of a single cavity and/or boreholes leads to a reduction in pressure head distribution, particularly under a hydraulic structure apron.

Figure 3 shows the streamlines for the cases of flow without a cavity and boreholes, with a single cavity and without boreholes, and with a single cavity and boreholes. It is clear from this figure that the presence of a cavity and/or boreholes leads to a reduction in exit gradient and downstream discharge. Also, it was observed that the presence of a cavity leads to an increase in the under-seepage. The results obtained from the mathematical model were used to calculate all the hydraulic properties mentioned above. The difference in the increase or decrease in the uplift pressure head, exit gradient, downstream

discharge, and under-seepage discharge was calculated using equations (4 to 7).

Table 3: *Comparison between FDM solution and experimental results for the case (L=10d1) and (b=0.5L)*

Preglednica 3: *Primerjava med rešitvijo FDM in eksperimentalnimi rezultati za primer (L = 10d1) in (b = 0,5L)*

Distance (X/L)	Without borehole		With borehole	
	Exp.	FDM	Exp.	FDM
0.0	0.74	0.75	0.63	0.65
0.1	0.71	0.72	0.56	0.58
0.2	0.65	0.66	0.46	0.47
0.3	0.59	0.60	0.34	0.34
0.4	0.57	0.57	0.18	0.18
0.5	0.51	0.51	0.00	0.00
0.6	0.47	0.46	0.11	0.10
0.7	0.42	0.41	0.14	0.13
0.8	0.36	0.35	0.16	0.14
0.9	0.30	0.30	0.15	0.14
1.0	0.27	0.26	0.14	0.13

Table 4 illustrates the relative change in the hydraulic properties, such as exit gradient, downstream discharge, and uplift pressure head, due to different values in the upstream head ratio *H/L* and different cavity locations. This table indicates that the upstream head ratio *H/L* has no significant effect on the reduction of the hydraulic properties. In contrast, the position of the cavity plays a crucial role in influencing the hydraulic properties. The distribution of water pressures is governed by the Laplace equation for steady-state flow, whereby the geometric boundaries of the internal cavity have a greater influence than the external shape of the hydraulic structure. Therefore, changing the *H/L* ratio without altering the internal soil structure has only a minor effect on the discharge and exit gradient, provided that the seepage length remains relatively constant. Conversely, the presence of a cavity in the porous layer beneath the hydraulic head acts as a preferential flow path, causing a sharp deflection in the equipotential lines and flow lines, thereby altering the distribution of pressure head. The negative values of the relative change in all hydraulic properties indicate that the presence of the cavity results in a decrease in all hydraulic characteristics. It has been noted that the greatest relative change in the exit gradient and downstream discharge occurs when the cavity is positioned directly beneath the center of the hydraulic structure floor. Conversely, the most significant relative change in the resultant uplift pressure is observed when the cavity is situated nearer to the upstream sheet pile.

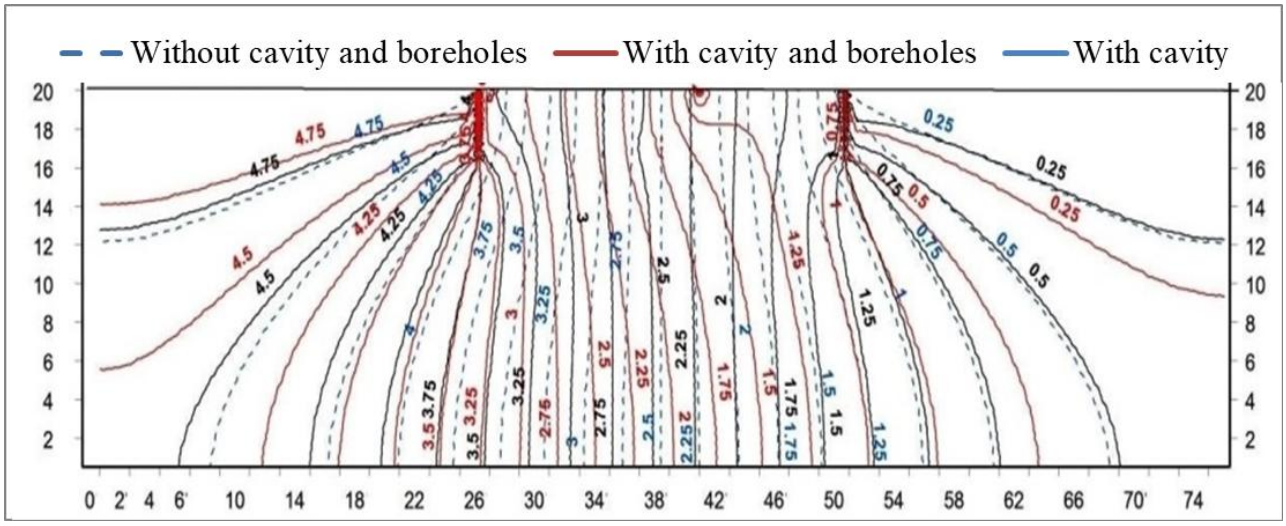


Figure 2: *The equipotential line map for H/L=0.2, W/L=0.04, Y/L=0.14, and b=0.65L.*

Slika 2: *Prikaz ekvipotencialnih črt za H/L=0,2, W/L=0,04, Y/L=0,14 in b=0,65L.*

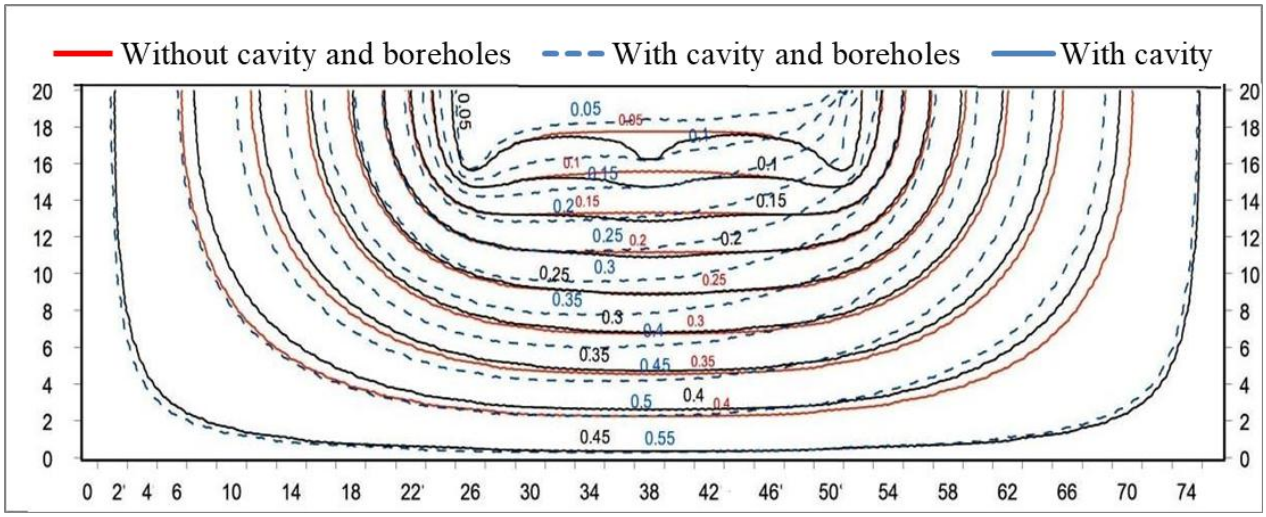


Figure 3: *The streamline map for H/L=0.2, W/L=0.04, Y/L=0.14, and b=0.65L.*

Slika 3: *Prikaz tokovnic za H/L=0,2, W/L=0,04, Y/L=0,14 in b=0,65L.*

Table 4: *The relative change in hydraulic properties due to different upstream water head and cavity locations and for Y/L=0.34, W/L=0.02.*

Preglednica 4: *Relativna sprememba hidravličnih lastnosti zaradi različnih gorvodnih vodostajev in različnih lokacij votlin ter za Y/L=0,34, W/L=0,02.*

X/L	ΔEG			ΔQd			ΔF		
	H/L=0.12	H/L =0.16	H/L =0.2	H/L =0.12	H/L =0.16	H/L =0.2	H/L =0.12	H/L =0.16	H/L =0.2
-0.74	-0.1870	-0.1870	-0.1870	-0.1925	-0.1923	-0.1921	-0.1436	-0.1439	-0.1436
-0.54	-0.2558	-0.2558	-0.2558	-0.2626	-0.2624	-0.2622	-0.1988	-0.1992	-0.1989
-0.34	-0.3567	-0.3567	-0.3566	-0.3644	-0.3642	-0.3640	-0.2840	-0.2843	-0.2840
-0.14	-0.4845	-0.4844	-0.4844	-0.4911	-0.4908	-0.4907	-0.3985	-0.3988	-0.3985
0.06	-0.5899	-0.5899	-0.5898	-0.5921	-0.5919	-0.5917	-0.4866	-0.4868	-0.4866
0.46	-0.6684	-0.6684	-0.6684	-0.6582	-0.6581	-0.6580	-0.4237	-0.4240	-0.4238
0.86	-0.5621	-0.5622	-0.5622	-0.6092	-0.6091	-0.6090	-0.2003	-0.2007	-0.2004
1.06	-0.3368	-0.3368	-0.3369	-0.5161	-0.5160	-0.5160	-0.0992	-0.0996	-0.0993
1.26	-0.1466	-0.1467	-0.1467	-0.3872	-0.3871	-0.3870	-0.0429	-0.0434	-0.0430
1.46	-0.0643	-0.0643	-0.0643	-0.2786	-0.2784	-0.2783	-0.0197	-0.0201	-0.0197
1.66	-0.0327	-0.0327	-0.0328	-0.2032	-0.2030	-0.2029	-0.0103	-0.0107	-0.0103
1.86	-0.0194	-0.0194	-0.0194	-0.1470	-0.1468	-0.1467	-0.0061	-0.0066	-0.0062

Figure 4 shows the relative changes (in percent) of the exit gradient for different cavity locations. It shows that the exit gradient decreases as the single cavity location moves from upstream to the end of the apron; the exit gradient increases at the end of the apron, reaching the downstream end. The maximum reduction occurs when the cavity is located at the mid-point of the apron and is equal to (-0.658), while the maximum increase occurs when the cavity is located at the far point of the downstream and is equal to (+0.147). Also, this figure shows that, as the depth of the single cavity increases, the decrease or increase in the exit gradient difference decreases.

Figure 5 shows the relative changes (in percent) of the downstream discharge for different cavity locations. The analysis indicates that a decrease in downstream discharge is observed for all positions of the single cavity, with the exception of one specific location at the downstream end, where Y/H equals 0.14. The maximum reduction occurs when the cavity is located at the mid-point of the apron and is equal to (-0.64), while the maximum increase occurs at the far point of the downstream end and is

equal to (+0.034). Also, this figure shows that the percentage of reduction decreases as the depth of the single cavity decreases.

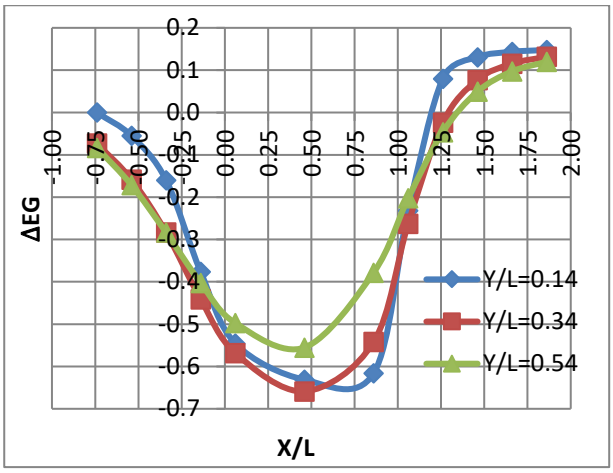


Figure 4: *The relative change of exit gradient (EG) in % for different cavity locations (X/L) and (Y/L); for H/L=0.16 and W/L=0.04.*

Slika 4: *Relativna sprememba izstopnega gradienta (EG) v % za različne lege votline (X/L) in (Y/L); za H/L = 0,16 in W/L = 0,04.*

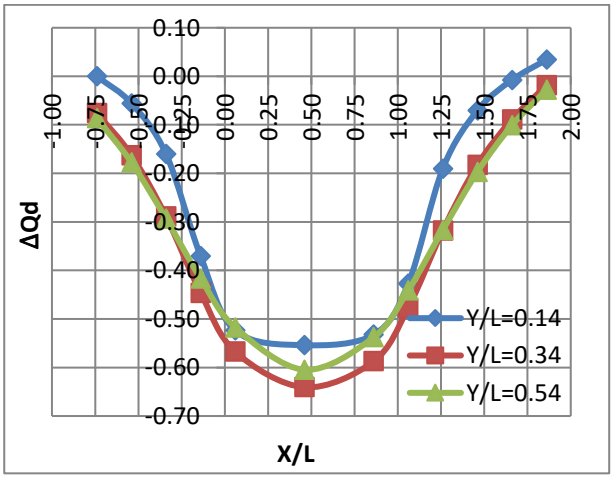


Figure 5: *The relative change of downstream discharge in % for different cavity locations (X/L) and (Y/L); for H/L=0.16 and W/L=0.04.*

Slika 5: *Relativna sprememba pretoka v spodnjem delu v % za različne lege votline (X/L) in (Y/L); primer H/L = 0.16 in W/L = 0.04.*

Figure 6 shows the relative changes in the uplift pressure head for different cavity locations. The reduction in uplift pressure head is observed as the position of the single cavity shifts from the upstream to the downstream end. The maximum reduction occurs when the cavity is located at the beginning point of the apron and is equal to (-0.674), while the minimum decrease occurs when the cavity is located at the far point of the downstream end and is equal to (-0.0022). Also, it is possible to follow the effect of the cavity depth on reducing the uplift pressure head along the problem domain. It is observed that, as the depth of the cavity increases, the reduction in the uplift pressure head increases up to the starting point of the hydraulic structure apron. At this point, there is a turnover where the reduction of the uplift pressure head starts decreasing as the depth of the cavity increases. This behavior is maintained to the end point of the hydraulic structure apron. Then this turnover is reversed starting from this point to the end of the problem domain, i.e., there is a direct relationship between the depth of the cavity and the reduction in the uplift pressure head.

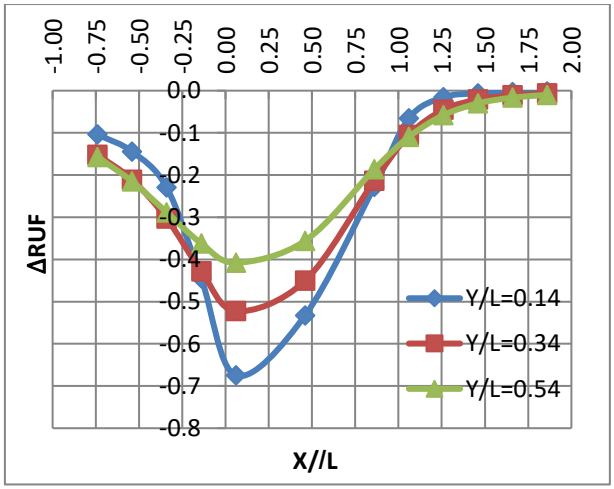


Figure 6: *The relative change of uplift pressure head in % for different cavity locations (X/L) and (Y/L); for H/L=0.16 and W/L=0.04.*

Slika 6: *Relativna sprememba višine vzgonskega tlaka v % za različne lege votline (X/L) in (Y/L); za H/L = 0,16 in W/L = 0,04.*

Figure 7 shows the relative changes in the exit gradient for different cavity sizes. The reduction in exit gradient is observed as the position of the single cavity shifts from the upstream area to the downstream end. The maximum reduction occurs when the cavity is located at the midpoint of the apron and is equal to (-0.704), while the minimum decrease occurs when the cavity is located at the far point of the downstream end and is equal to (-

0.0184). Also, this figure shows that, as the size of the single cavity increases, the reduction in the exit gradient increases. Figure 8 shows the relative changes in the downstream discharge for different cavity sizes. The reduction in downstream discharge is observed to increase as the position of the single cavity shifts from the upstream area to the downstream end. The maximum reduction occurs when the cavity is located at the midpoint of the apron and equals (-0.69), while the minimum decrease occurs at the far point of the downstream and is equal to (-0.14). Also, this figure shows that, as the size of the single cavity increases, the reduction in the downstream discharge also increases.

Figure 9 shows the percentage decrease in the uplift pressure head for different cavity sizes. As the position of the single cavity shifts from upstream to downstream, a reduction in uplift pressure head is observed. The maximum reduction occurs when the cavity is located at the first quarter of the apron and is equal to (-0.522), while the minimum decrease occurs when the cavity is located at the far point of the downstream end and is equal to (-0.006). Also, this figure shows that, as the size of the single cavity increases, the reduction in the uplift pressure head increases.

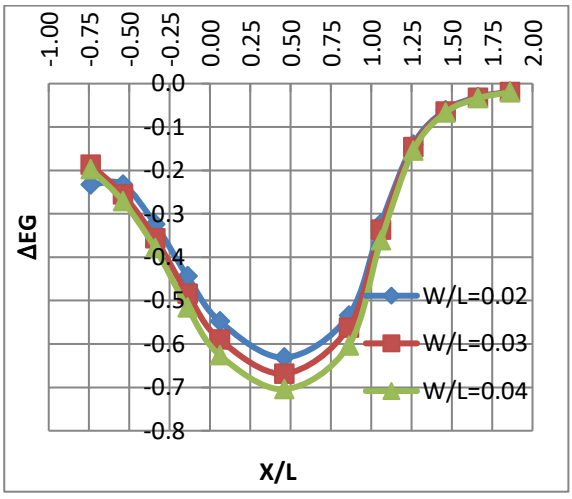


Figure 7: *The relative change of exit gradient in % for different cavity sizes; for H/L=0.2 and Y/L=0.34.*

Slika 7: *Relativna sprememba izstopnega gradienta v % za različne velikosti votline; za H/L = 0,2 in Y/L = 0,34.*

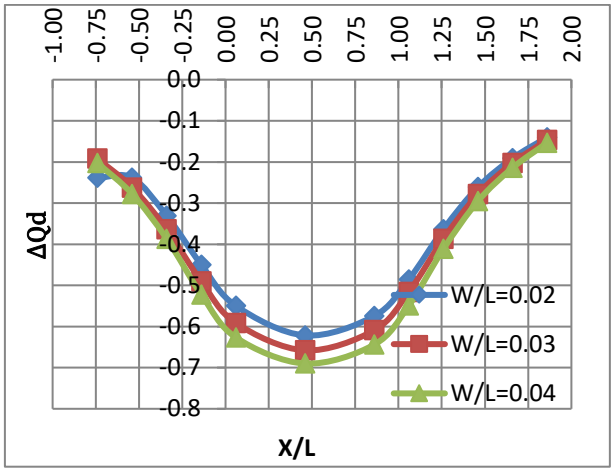


Figure 8: *The relative change of downstream discharge in % for different cavity sizes; for H/L=0.2 and Y/L=0.34.*

Slika 8: *Relativna sprememba dolvodnega pretoka v % za različne velikosti votline; za H/L = 0,2 in Y/L = 0,34.*

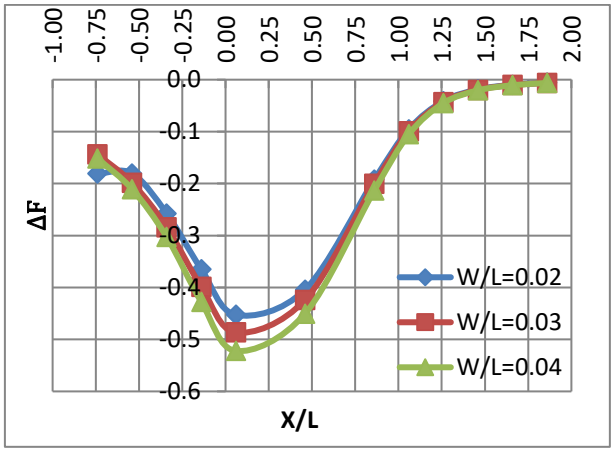


Figure 9: *The relative change of uplift pressure head in % for different cavity sizes; for H/L=0.2 and Y/L=0.34.*

Slika 9: *Relativna sprememba višine vzgonskega tlaka v % za različne velikosti votline; za H/L = 0,2 in Y/L = 0,34.*

Figure 10 shows the relative changes in the under-seepage discharge for different cavity sizes. The reduction in under-seepage discharge is observed as the position of the single cavity shifts from the upstream area to the end of the apron. Subsequently, an increase in under-seepage discharge is noted when the cavity is situated at the apron's end, continuing to rise as it approaches the downstream limit. The maximum reduction occurs when the cavity is located at the end point of the apron and is

equal to (-0.68), while the maximum increase occurs when the cavity is located at the start portion of the downstream end and is equal to (+0.344). Also, this figure shows that, as the size of the single cavity increases, the decrease in the under-seepage discharge also increases, while the size of the cavity has no clear effect on increasing the under-seepage discharge at the downstream portion.

Figure 11 shows the relative changes in the under-seepage discharge for various cavity locations. The reduction in under-seepage discharge is observed as the position of the single cavity shifts from the upstream area to the end of the apron. Subsequently, an increase in under-seepage discharge is noted when the cavity is situated at the apron's end, continuing to rise as it approaches the downstream limit. The maximum reduction occurs when the cavity is located at the end point of the apron and is equal to (-0.711), while the maximum increase occurs when the cavity is located at the start portion of the downstream end and is equal to (+0.38). Also, this figure shows that, as the depth of the single cavity increases, the reduction and increase in the under-seepage discharge increase.

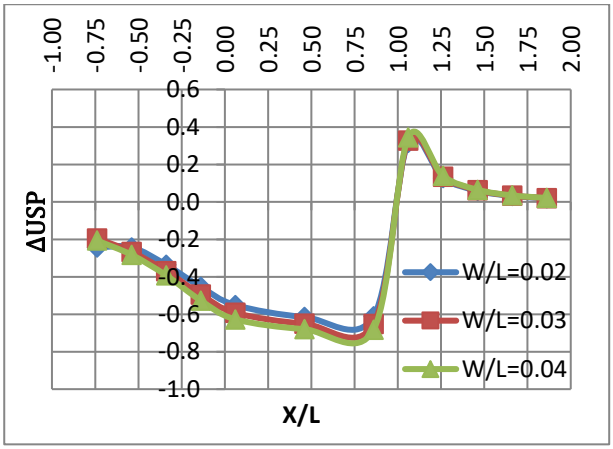


Figure 10: *The relative change of under-seepage discharge in % for different cavity sizes; for H/L=0.2 and Y/L=0.34*

Slika 10: *Relativna sprememba pretoka podtekanja v % za različne velikosti votline; za H/L = 0,2 in Y/L = 0,34*

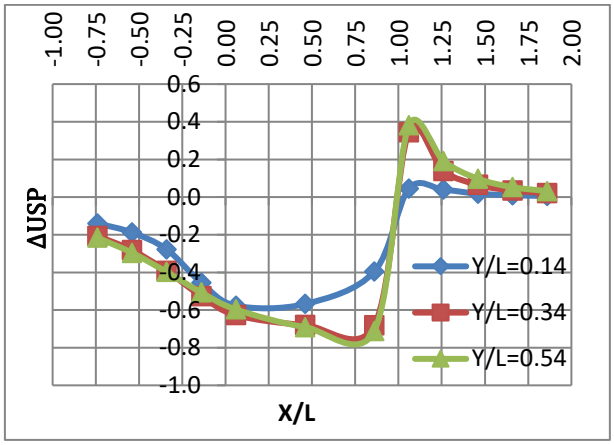


Figure 11: *The relative change of under-seepage discharge in % for different cavity locations; for W/L=0.04 and H/L=0.16.*

Slika 11: *Relativna sprememba pretoka podtekanja v % za različne lege votlin; za W/L = 0,04 in H/L = 0,16.*

Under-seepage Discharge Reduction in Terms of Boreholes

Under-seepage refers to the movement of water through porous foundations beneath hydraulic structures, influenced by differences in hydraulic head. This phenomenon involves deep seepage that penetrates into lower strata, moving away from the downstream toe. It was noted from the obtained results that the presence of cavities in the soil under the hydraulic structure mostly led to a decrease in all considered hydraulic property values, except for the under-seepage discharge. It was observed that the presence of cavities in certain locations in the soil leads to an increase in under-seepage discharge and thus to the loss of significant amounts of water in the soil. For this reason, a single borehole is used in the downstream floor of a hydraulic structure to reduce the amount of under-seepage discharge. Three locations were selected for the boreholes 0.5*L*, 0.65*L*, and 0.75*L* to study their effect on reducing the under-seepage discharge.

Figure 12 shows the relative changes in the under-seepage discharge for different borehole locations. It is observed that using boreholes in the hydraulic structure apron leads to a reduction in under-seepage discharge for all locations of the boreholes and cavities. When the cavity is located at the downstream end of the apron, the maximum

difference reduction appears to be (0.326-0.076=+0.25), while the minimum difference reduction appears to be (-0.68-(-0.65)=-0.03). This figure further shows that the location of the single boreholes has less effect on the reduction in the under-seepage discharge.

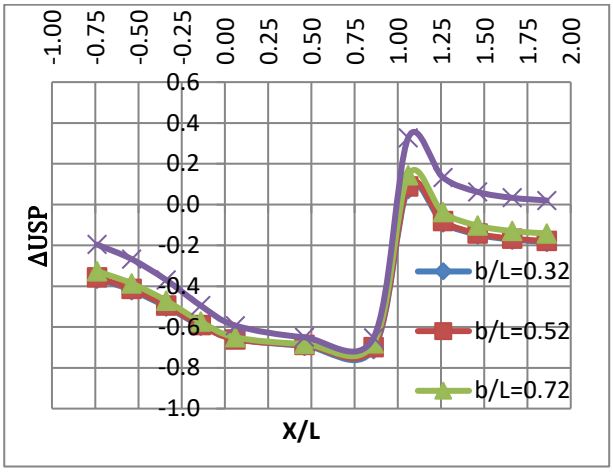


Figure 12: *The relative change of under-seepage discharge in % for different boreholes locations; for W/H=0.03, Y/L=0.34, and H/L=0.16.*

Slika 12: *Relativna sprememba pretoka podtekanja v % za različne lokacije vrtin; za W/H = 0,03, Y/L = 0,34 in H/L = 0,16.*

6. Conclusion

From the above results, the following conclusions can be drawn:

- The presence of a single cavity under hydraulic structures generally leads to a reduction in downstream discharge, uplift pressure head, and exit gradient, while it leads to a decrease or increase in the under-seepage discharge depending on the location of the single cavity.
- The maximum value for reducing the exit gradient and downstream discharge occurs when the single cavity is located under the middle of the hydraulic structure apron. On the other hand, the maximum increase occurs for the above characteristics when a single cavity is located at the downstream end of the domain.
- The maximum reduction of the uplift pressure head occurs when a single cavity is located under the first (upstream) quarter of the hydraulic structure apron.
- The maximum change of the under-seepage discharge occurs when the single cavity is located under the fourth (downstream) quarter of the hydraulic structure apron.
- The location of the single cavity has a greater effect than the size of the cavity in reducing or increasing the above hydraulic properties.
- Drilling the boreholes in the hydraulic structure apron leads to a decrease in all considered hydraulic properties.

The practical implications of the findings can be categorized into three key areas. Firstly, in design, it is advisable to incorporate natural cavities in the central region of the embankment toe, as these cavities effectively relieve uplift pressure and gradient at the outlet without exacerbating seepage issues. In contrast, voids at the lower end of the structure should be avoided, as they can lead to concentrated flow outlets that increase discharge and gradient problems. Secondly, in terms of assessment and predictive analysis, the positioning of cavities serves as a qualitative indicator of potential hazards; a cavity in the central area suggests normal pressure relief, while one near the toe signals a critical hazard that necessitates prompt intervention to avert piping. Lastly, for maintenance and monitoring, geophysical surveying (GPR) and grouting should be prioritized in the lower section where cavities pose the greatest risk, whereas those in the central area should be included in regular monitoring schedules.

Acknowledgments

The authors would like to express their gratitude to the colleagues who provided assistance with language editing and manuscript proofreading.

CRediT authorship contribution statement

Ihsan A. Abdulhussein: Conceptualization, Methodology, Formal analysis, Investigation, Writing – original Fortran code, Supervision, Corresponding author. Rafi M. Qasim: Investigation, Resources, Data curation. Saja M. Naeem: Data curation, Visualization, Writing –

review & editing. K. S. Hari Prasad: Project administration, Writing – review & editing.

Data availability

All scientific research data and numerical results used in this study are preserved by the authors and are available upon reasonable request and at . The modeling results obtained using Fortran 90 Software using the code designed, implemented, and performed by the authors are available at https://zenodo.org/records/22261772. For additional information or to request modeling files, please contact the corresponding author.

Declaration of interest

The authors declare that they have no known financial or personal conflicts of interest that could have appeared to influence the work reported in this paper. No generative AI tools were used in the writing or preparation of this manuscript

Funding

This research did not receive any specific grant from funding agencies in the public, commercial, or not-for-profit sectors.

References

Abdallah M. H. (2017): The Influence of Cavities on the Stability of Dam During Water Flow. M.Sc. Thesis, University of Kufa, Iraq.

Ali, L., and Tanaka, N. (2023). Experimental Investigation of Levee Erosion during Overflow and Infiltration with Varied Hydraulic Conductivities of Levee and Foundation Properties in Saturated Conditions, *GeoHazards*, Vol. 4, 286–301.

Aziz. L. J, & Abdallah, M. H. (2018). Suitable Location of Sheet Pile under Dam Resting on Sandy Soil with Cavity, *Kufa Journal of Engineering*, Vol. 9, No. 2 , 168-188

Baena, C.M. and Toledo, M.A. (2014). An experimentally verified model of the seepage progress due to dissolution of soluble particles in foundations subject to intergranular flow, *Environ. Earth Sci.*, Vol. 72, 3369–3382.

Bear, J., (1979). *Hydraulics of Ground Water*, Mc. Graw-Hill, New York.

Cedergren, H. R. (1989). *Seepage, Drainage, and Flow Nets* (3rd ed.). Wiley.

Jamel A.A. and Ali M.I. (2018). Influence of Cavity Under Hydraulic Structures on Seepage Characteristics, *Int. J. Engineering & Technology*, 7(4.20), 464-471.

Chawla, A. S. (1976). Effect of drains on pressure below structures, *Journal of Geotechnical Engineering Division, ASEC*, Vol. 102, No. GT1, pp.15-29.

Hameed, I. H., Al-Shukur, A. K., and Hassnen Mosa Jafer, H. M., (2025). Experimental and Numerical Investigation of Seepage and Seismic Dynamics Behavior of Zoned Earth Dams with Subsurface Cavities, *GeoHazards*, Vol. 6, No. 37. https://doi.org/10.3390/

Maatooq J.S., Laith J. Aziz, Taghreed A. Almahdee Musa. (2014). Development of Empirical Formula for Influence of Cavities on Seepage under Sheet Pile Wall for Hydraulic Structures. *Kufa journal of Engineering* Vol.5, No.2, 93-106.

Maatooq, J. S. and Abdulhasan, D. M. (2019). Impact of Cavitation within the Homogeneous Soil under hydraulic Structure on Formulation of the Seepage Quantity and Uplift Pressure, *International Journal of Civil Engineering and Technology*, Vol.10, Issue 01, 640-650.

Nadhir, A.-A., Nasrat, A., Varoujan, S. Sven, K., and Jan, L. (2017). Is Mosul Dam the Most Dangerous Dam in the World? Review of Previous Work and Possible Solutions, *Engineering*, Vol. 9, 801–823.

Remson, I., Hornberger, G. M, and Molz, F. D., (1971). *Numerical methods in subsurface hydrology*. John Wiley, New York.